Carcinogenesis vol.29 no.3 pp.491–499, 2008
doi:10.1093/carcin/bgm246
Advance Access publication January 19, 2008

PPP1CA contributes to the senescence program induced by oncogenic Ras

Maria E.Castro[1], Irene Ferrer[1], Alberto Cascón[2], Maria V.Guijarro[1,4], Matilde Lleonart[3], Santiago Ramon y Cajal[3], Juan F.M.Leal[1], Mercedes Robledo[2] and Amancio Carnero[1,*]

[1]Experimental Therapeutics Programme, [2]Human Genetics Programme, Spanish National Cancer Research Center (CNIO), 28029 Madrid, Spain and [3]Departamento de Patología, Hospital Vall d'Hebron, Barcelona, Spain

[4]Present address: Experimental Pathology Program, Department of Pathology, New York University School of Medicine, 550 First Avenue, NY 10016 USA

*To whom correspondence should be addressed. Tel: +917 328 021; Fax: +917 328 051;
Email: acarnero@cnio.es

Ectopic expression of conditional murine p53 (p53val135) and oncogenic *ras* is enough to induce a senescent-like growth arrest at the restrictive temperature. We took advantage of this cellular system to identify new key players in the *ras*/p53-induced senescence. Applying a retroviral-based genetic screen, we obtained an antisense RNA fragment against PPP1CA, the catalytic subunit of protein phosphatase 1α, whose loss of function bypasses *ras*/p53-induced growth arrest and senescence. Expression of a specific short hairpin (sh)RNA against PPP1CA impairs the p53-dependent induction of p21 after DNA damage and blocks the subsequent pRb dephosphorylation, thus bypassing p53-induced arrest. We found that oncogenic *ras* promotes an increase in the intracellular level of ceramides together with an increase in the PPP1CA protein levels. Addition of soluble ceramide to the cells induced a senescence phenotype that is blocked through PPP1CA downregulation by specific shRNA. Analysis of human tumors suggests that one of the PPP1CA alleles might be lost in a high percentage of carcinomas such as kidney and colorectal. The overexpression of two out of five PPP1CA alternative spliced variants reduced tumor cell growth and the downregulation of the protein to hemizygosity increased the anchorage-independent growth. We propose that oncogenic stress induced by *ras* causes ceramide accumulation, therefore, increasing PPP1CA activity, pRb dephosphorylation and onset of the p53-induced arrest, contributing to tumor suppression.

Introduction

Ras can induce transformation of established immortal but not primary mammalian cells. In primary cells, ectopic expression of oncogenic ras leads instead to a senescence-like state (1). Experiments using mutated alleles of ras unable to activate each of its downstream effectors have identified the mitogen-activated protein kinase signaling pathway as critical for ras-induced senescence (2). Ectopic overexpression of other oncoproteins located downstream of Ras in the mitogen-activated protein kinase effector pathway, such as Raf or MEK, also induces growth arrest (2,3).

Oncogenic activation of the Ras pathway in murine fibroblasts initiates a permanent cell-cycle arrest that depends on functional p53 and is phenotypically similar to replicative senescence (1,2,4) which is the cellular senescent state reached by increasing population doublings in primary somatic cells. The signaling from aberrant Ras activity to p53 is not fully understood, and the available data support a simple linear model through Ras induction of p19ARF (2,4,5). p19ARF links oncogene activation to the p53 tumor suppressor pathway by inhibiting the Mdm2-dependent degradation of p53 (6,7). However, activation of the ARF/p53 pathway results in apoptosis or senescence, depending on the cell type and oncogenic stress (8), implying that additional signals can modulate the outcome of the p53 activation (4). Oncogenic Ras and p53 cooperate to induce cell-cycle arrest, but after several days of this arrest a substantial portion of the cells are unable to reenter the cell cycle even when p53 activity has been removed (4,9). This observation suggests that p53 is required to initiate the cell-cycle arrest but that maintenance of the senescent state is partially independent of p53 and relies upon a *ras*-induced signal different from p21waf1 and p16ink4a (9).

To search for new regulators of senescence that can induce permanent p53-dependent cell-cycle arrest, we took advantage of the mouse temperature-sensitive p53 (p53val135) that allows conditional and reversible activation of p53. Using this model, we have followed a systematic approach to identify genetic events that inhibit the cellular senescence induced by the cooperation of oncogenic *ras* and p53 tumor suppressor. Applying a retroviral-based genetic screen, we obtained a messenger RNA (mRNA) antisense fragment against PPP1CA, whose loss of function bypasses p53-induced growth arrest. Expression of specific shRNA against PPP1CA impairs the p53 ability to induce p21 and blocks the pRb dephosphorylation. Downregulation of PPP1CA also enhanced the malignant properties of tumoral cells. On the contrary, overexpression of PPP1CA reduced the growth of tumor cells. Our data show that PPP1CA could behave as a tumor suppressor in human cells through its contribution to ras-induced senescence.

Abbreviations: MEF, mouse embryo fibroblast; mRNA, messenger RNA; PCR, polymerase chain reaction; PP1α, protein phosphatase 1α; RT, reverse transcriptase; shRNA, short hairpin RNA.

Materials and methods

Cell culture, retroviral vectors and gene transfer

Cells were generated and characterized following the same experimental procedure described in (9).

Generation of the antisense library

mRNA was extracted from mouse embryo fibroblasts (MEFs) terminally arrested at replicative senescence. Aliquots of 2 μg of total mRNA were used for the generation of the library. Randomly primed cDNA fragments of the poly-A+ mRNA were synthesized, size selected (50–500 bp) on a S400 column (Pharmacia) and cloned into the EcoRI and XhoI sites of pMARXIVpuro in the antisense orientation.

Retroviral-mediated antisense library transfer and *in vitro* recovery of the proviruses were performed as previously indicated in (10).

Temperature shifts and cell proliferation analysis

Cells were seeded at low density (6×10^4 cells/10 cm dish) in two sister plates and grown at either 32°C or 39°C. After 15 days in culture, we compared the number of colonies between the plate kept at 32°C and the sister plate grown at 39°C.

Design of shRNA against PPP1CA

An shRNA against PPP1CA was designed using the 'Ambion siRNA target finder' and the 'Qiagen siRNA design tool' to choose the appropriate hairpin oligonucleotides, which were then cloned in a pRetrosuper vector.

Northern blot

Total RNA was extracted using RNAzolB. Ten micrograms of total RNA were run in formaldehyde–agarose gels and transferred to a Hybond membrane. The membrane was prehybridized during 4 h at 65°C. The probe was labeled by polymerase chain reaction (PCR) with 50 μC of redivue deoxycytidine triphosphate^{32} (Amersham), using specific primers for mouse PPP1CA. The purified probe was denatured and added to the hybridization solution. The hybridization was performed overnight at 65°C. After extensive washing, the membrane was exposed to a Biomax MS film (Kodak).

Immunoblotting

Immunoblotting was performed as previously indicated in (10,11). To detect the different proteins, membranes were hybridized with the primary antibody [anti-PP1α (protein phosphatase-1α) from Calbiochem; anti-Rb: G3-245 from BD PharMingen; anti-p53: sc-6243, anti-p21: sc-397 and anti-Bax: sc-493 from Santa Cruz; and anti-α-tubulin: T9026 from Sigma].

NIH cells treatment with doxorubicin and H_2O_2

NIH cells stably transduced with either PPP1CA antisense or pMARXIVpuro empty vector were seeded in six-well plates. Next day, cells at 50–75% confluence were treated with doxorubicin (0.4 or 0.8 μg/ml), during 8 or 24 h or with 100 μM H_2O_2, during 6 h. After this period of time, cells were harvested as described in Immunoblotting.

Determination of ceramide intracellular levels by thin layer chromatography

Cells (25×10^4 cells per well) were seeded on six-well plates in triplicates. Cells were incubated for 2 days at 39°C in the presence of 1 μCi/ml of [^{14}C]serine. Then, samples of conditions due at 39°C were washed once with phosphate-buffered saline and plates were frozen at −80°C. Regarding samples at 32°C, after adding 1 ml of additional fresh medium, plates were kept 16 h at 32°C. Afterwards, cells were washed once with phosphate-buffered saline and frozen at −80°C. Lipids were harvested by a solution based on chloroform:methanol:water (30:15:3, vol:vol:vol). The organic phase was dried in a concentrator under N_2 flow at 37°C. Samples were resuspended in chloroform:methanol (1:1, vol:vol) and lipids separated by thin layer chromatography in chloroform:methanol:ammonium (2 M) (65:25:4, vol:vol:vol). Quantification of lipids was carried out by Instantimager.

Exogenous ceramide addition

In all, 1 00 000 p53−/−;ts cells (C4) or p53−/−;ts cells transduced with PPP1CA shRNA (C4ligP4) were seeded on six-well plates. After 24 h at 39°C, plates were placed at 32°C for 2 h before addition of 10 μM C_6-ceramide (*N*-hexanoylsphingosine) and were kept at 32°C since then. Forty-eight hours after the first addition, fresh medium with new C_6 (10 μM) was added to the cells. Seventy-two hours after the first ceramide addition, cells were fixed with 0.5% glutaraldehyde in phosphate-buffered saline. Under the microscope, senescent morphology was assessed.

Dot blot

The Cancer Profiling Array membrane (BD Biosciences) was hybridized as previously reported (12). The probe was labeled by PCR with 50 μC of redivue deoxycytidine triphosphate^{32} (Amersham), using specific primers for human PPP1CA. The labeled probe was then purified from free hot nucleotides with a sepharose G-50 column Nick^{TM}. The hybridization was performed overnight at 65°C.

PCR of the different splicing variants of PPP1CA

To verify the existence of the different splicing variants of PPP1CA in our system, specific reverse transcriptase (RT)–PCRs were performed. The primers used were the following: SP1 Fw: 5′ AGGAGAGCCAGGCCGGAAGG3′; SP1 Rev: 5′TGATGTGCTCTGCAGATGAGGTCC3′; SP3 Fw: 5′CGGAGCGGCGGCGCCGCCAT3′; SP3 Rev: 5′GGGGTGTGGTAATCTCCCCTAATAAG3′; SP5 Fw: 5′AGCGGCGGCGCCGCCATGTC3′; SP5 Rev: 5′GCTCTACCCTCATCTACCTTCCAG3′ and for SP0, Fw: 5′CGGAGCGGCGGCGCCGCCAT3′ and Rev: 5′GCACATGGAGGCTATTTCTTGGC3′.

Overexpression of different splicing variants of PPP1CA

HCT116 p53−/− cells were transfected. After 16 h, a glycerol shock was performed and cells were cultured at 37°C. Forty-eight hours after transfection, cells were selected with 0.5 μg/ml of puromycin. Twelve days after, plates were fixed and colonies stained with crystal violet.

Growth in soft agar

To measure the anchorage-independent growth, we follow a protocol described previously in (11). Colonies were scored 3 weeks after seeding and all values were determined in triplicate.

Quantitative RT–PCR

Quantitative RT–PCR was essentially performed as described in (12). Normal and tumor tissues from 20 patients with lung carcinoma were randomly chosen from the tumor bank at the Pathology Department of Vall d'Hebrón Hospital (Barcelona, Spain). Quantitative real-time TaqMan RT–PCR technology (Applied Biosystems, Foster City, CA) was used to determine the differential expression of the selected genes. Cyclophilin (ref. 4326316E), an endogenous control, was used to normalize variations in cDNA quantities from different samples. Each reaction was performed in triplicate with cDNA from normal and tumor tissues from each patient studied. A new RNA extraction was randomly performed from the original tissue of some samples and reproducible quantitative real-time PCR results were obtained (data not shown).

Multiplexed genomic loss detection

To investigate the presence of deletions affecting the *PPP1CA* gene, we used a technique based on specific multiplex amplification of the gene as previously reported in (13). We first designed and labeled (5′ 6-FAM) one pair of primers for each exon. The primer pairs for amplification were designed on the basis of genomic sequences of *PPP1CA*. We used control fragments from chromosome 11 as internal controls of the assay.

Results

Loss-of-function genetic screening

We have performed a large-scale genetic screen to identify genes whose loss of function bypasses the *ras*-dependent senescent phenotype in our cellular system. Our system, consisting of p53−/−;ts-ras and p53−/−;p21−/−;ts-ras cells which carry oncogenic *ras* and a thermosensitive mutant of p53, undergoes terminal growth arrest with features of senescence when the temperature is switched to 32°C (9).

A random antisense fragment library generated from total polyA+ mRNA was cloned into the murine moloney leukemia virus-based retroviral vector pMARXIVpuro. This library contained $\sim 6 \times 10^6$ independent clones. The library was transfected into ecotropic retrovirus–packaging cells and the replication-deficient viruses generated were then infected into exponentially growing p53−/−;p21−/−;ras;ts cells (39°C). Following selection for puromycin resistance during ∼6 days, cells were plated at low density and shifted to 32°C. After 2 weeks, colonies that had overcome ras/p53-induced senescence were identified and the genomic DNA was extracted from individual clones (Figure 1a). Independent provirus-carrying individual antisense fragments were retested and positive fragments identified by comparison with the BLAST database.

Among other antisense fragments, we recovered, at least twice in an independent form, antisenses against p53 mRNA. These antisenses map into a short p53 region previously reported as being efficient for mRNA antisense activity (10). These antisense fragments represent a validation for our genetic screening.

In the screening, we identified an antisense against PPP1CA. The antisense fragment was 133 nt long, which is around the size that has been reported as being the most effective for gene silencing (10). The antisense is located at the end of the coding sequence of the mRNA (Figure 1b) and its expression in the p53−/−;ts-ras and p53−/−;p21−/−;ts-ras cells bypass the p53/ras-induced senescent arrest (Figure 1c). Quantification of the level of bypass indicated that PPP1CA antisense expression allows ∼50% colony formation compared with the same cells growing at 39°C. Similar bypass was observed in p53−/−;ts cells at 32°C (data not shown). Therefore, the PPP1CA antisense fragment significantly induced cellular growth, bypassing the p53-induced cell-cycle arrest and senescence.

To additionally confirm that the effect observed with the antisense fragment was due to PPP1CA inactivation, and not to unspecific matching, we analyzed the effect of several shRNA against mouse PPP1CA in the same system. We designed and tested six different shRNAs; however, only one of them produced significant reduction of PPP1CA protein (Figure 1d). The designed shRNA only reduced PPP1CA protein level to one half when introduced in p53−/−;ts;ras cells. Nevertheless, this partial reduction of PPP1CA protein allowed a significant increase in cellular growth at the permissive temperature (Figure 1e), bypassing the p53-induced cell-cycle arrest to a level similar to the one obtained with antisense fragment. No effect was observed when p53−/−;ts;ras cells were infected with the pRS empty vector or several other shRNAs which did not reduce the PPP1CA protein level (data not shown).

PPP1CA protein increases in a Ras-dependent fashion

It has been proposed that PP1α enzymatic activity is regulated by Ras (14) and a correlation between Ras activation and PP1/PP2A activation has also been previously reported (15). We analyzed PPP1CA mRNA levels by northern blot and its maximum levels of expression did not correlate with Ras expression, either in p53−/−;ts;ras MEFs or in wild-type MEFs expressing Ras-v12 (Figure 2a). Nevertheless, the analysis of PPP1CA protein levels revealed a Ras-dependent

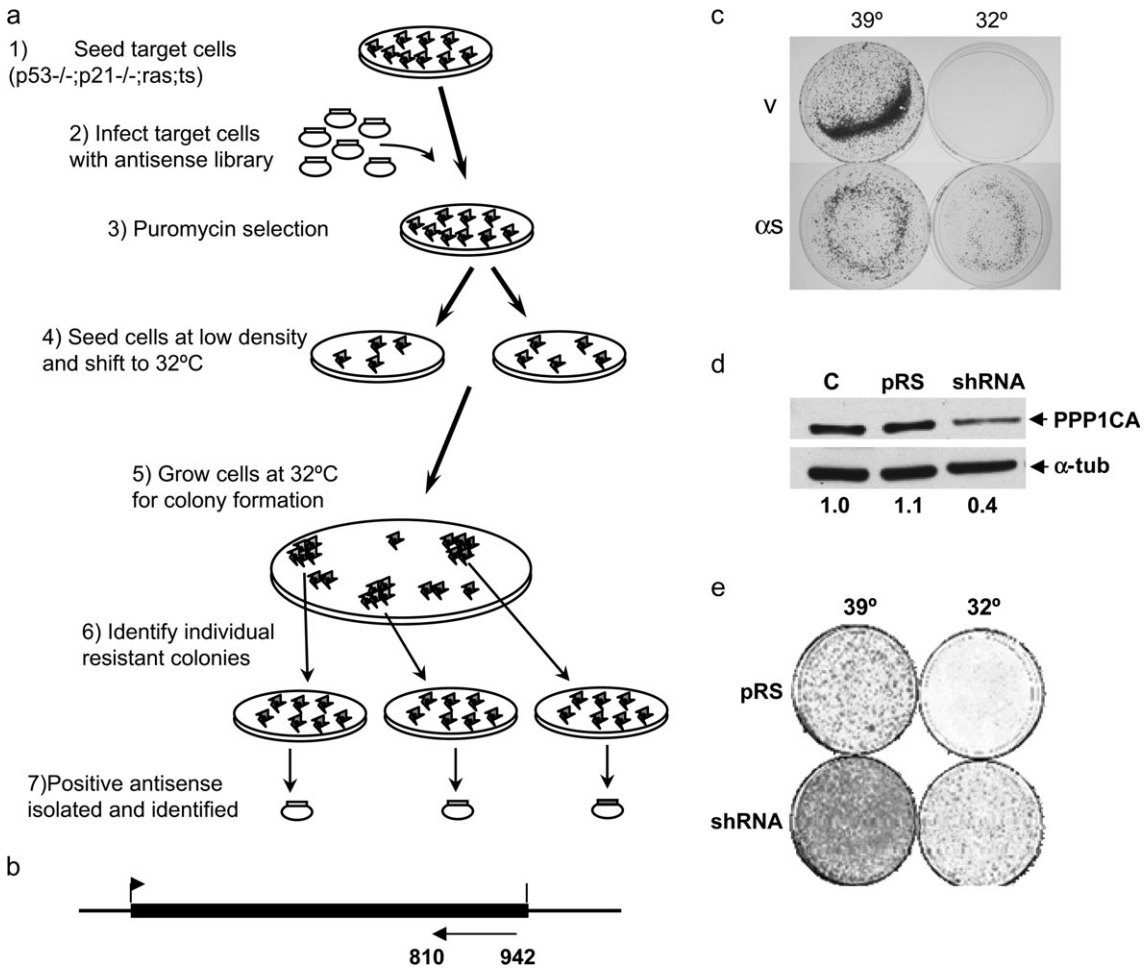

Fig. 1. (**a**) Scheme of the loss-of-function screening. (**b**) Scheme of the location and size of the PPP1CA antisense fragment identified compared with the PPP1CA mRNA transcript. (**c**) Antisense fragment against PPP1CA inhibits p53-induced growth arrest. In all, 6×10^4 p53−/−; ts-ras cells carrying the antisense fragment (αs) or vector alone (v) were grown at restricted temperature (39°C) or permissive temperature (32°C) during 2 weeks. Then, cells fixed with glutaraldehyde 0.5% and stained with 1% crystal violet to visualize colony growth. (**d**) Effect of the shRNA against PPP1CA and analysis of PPP1CA mRNA and protein levels in our system. p53−/−;ts-ras cells carrying the shRNA against PPP1CA (shPNA) or vector alone (pRS) were grown at restricted temperature (39°C). Cells were starved and protein levels analyzed by immunoblotting. (**e**) shRNA against PPP1CA was able to induce growth at permissive temperature (32°C) in p53−/−;ts-ras cells. In all, 6×10^4 p53−/−;ts-ras cells carrying the shRNA against PPP1CA (shRNA) or vector alone (pRS) were grown at restricted temperature (39°C) or permissive temperature (32°C) during 2 weeks. Then, cells fixed with glutaraldehyde 0.5% and stained with 1% crystal violet to visualize colony growth.

increase both in p53−/−;ts;ras MEFs and in p53−/− MEFs expressing Ras-v12 (Figure 2b). Our data show a post-translational regulation of PPP1CA protein by oncogenic *ras* that causes an increase in the total levels of the protein.

Downregulation of PPP1CA impairs the p53 transcriptional response to doxorubicin and H_2O_2

Our system is p53 dependent; therefore, we measured the effect of PPP1CA shRNA on the induction of p53 by different stress agents. To that end, NIH3T3 cells transduced with either PPP1CA shRNA or empty vector were treated with doxorubicin at different times and concentrations. Afterwards, the levels of p53 and p21 were analyzed by western blot. As expected, p53 levels increased after doxorubicin treatment in cells transduced with either PPP1CA shRNA or empty vector (Figure 2c). Nevertheless, although p21 levels increased in NIH3T3 cells transduced with empty vector, this effect was impaired in cells stably expressing PPP1CA shRNA (Figure 2c).

NIH3T3 cells were also treated with H_2O_2, and the level of p21 was analyzed by western blot. We observed an increase in p21 protein level after 100 μM H_2O_2 treatment in NIH3T3 cells carrying only the empty vector, but in NIH3T3 cells expressing PPP1CA shRNA, p21 protein did not increase compared with the control without treatment (Figure 2d). In non-stimulated cells carrying the PPP1CA shRNA, p21 levels were higher than in empty vector cells. It is possible that the reduction of PP1 activity is sensed by the cell as some sort of stress, inducing a p53 response and therefore increasing p21 levels.

shRNA against PPP1CA can shift the phosphorylation state of Rb

PP1α has been identified as the protein phosphatase responsible for the dephosphorylation of pRb (16) and this has been related with the growth arrest response (17–19). Therefore, we sought to test whether partial inhibition of PPP1CA by expression of an shRNA would affect the behavior of pRb in our system.

In actively growing cells, the hyperphosphorylated form of Rb protein (ppRb) is the predominant one. On the contrary, when cells are delayed in their growth, the hypophosphorylated form of Rb protein (pRb) is the most abundant. In immortalized MEFs supplemented with insulin or in p53−/−;ts-ras cells growing at 39°C, the predominant pRb form was the hyperphosphorylated. On the contrary, MEFs deprived of serum showed enrichment in the hypophosphorylated form of pRb (Figure 2e and f). When p53−/−;ts-ras cells were shifted at 32°C, pRb became hypophosphorylated, in accordance with the growth arrest induced by thermosensitive p53 at this permissive

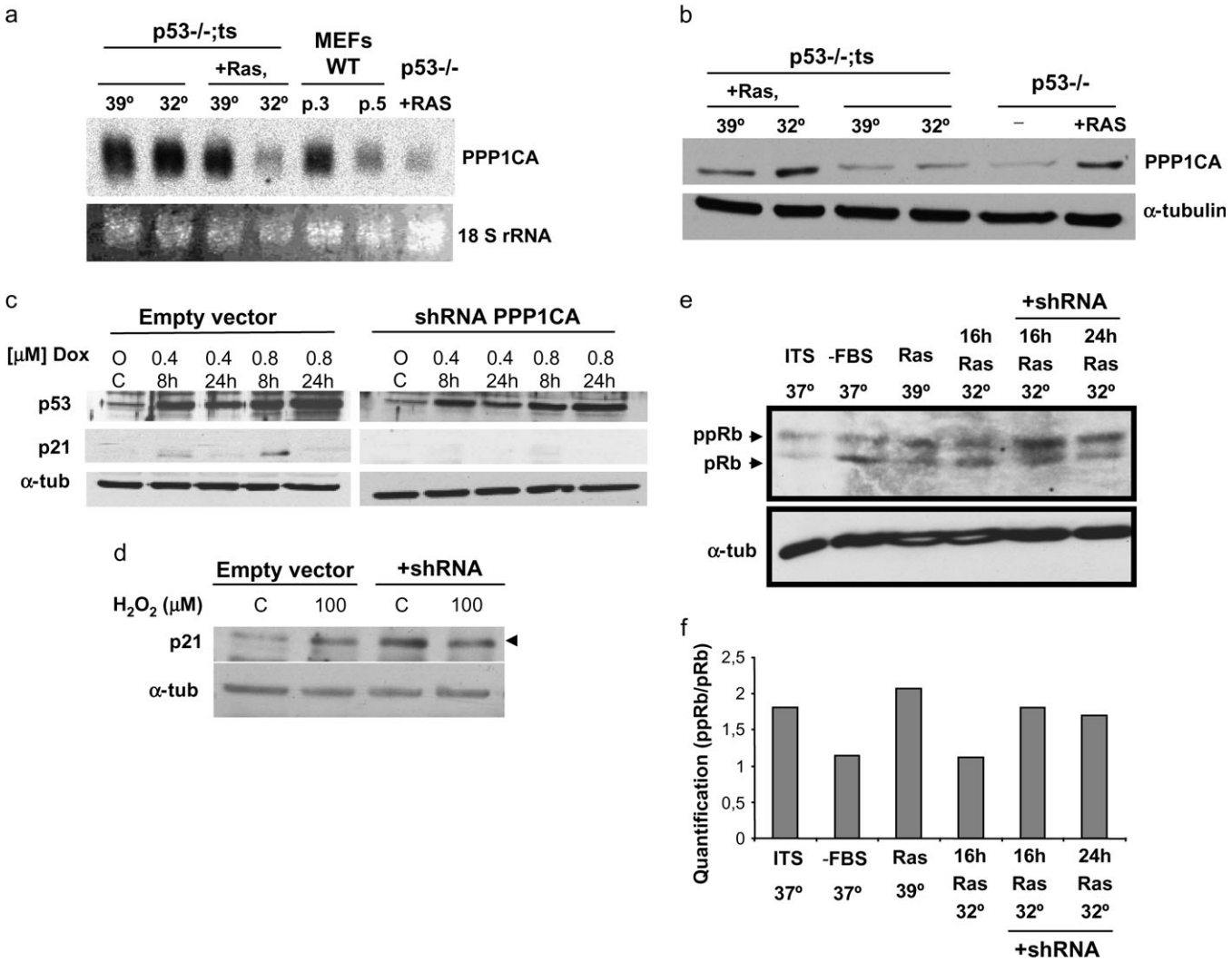

Fig. 2. (**a**) PPP1CA mRNA levels were not dependent on the expression of oncogenic ras. mRNA levels were analyzed by northern blot. A labeled probe able to specifically recognize PPP1CA isoform was used as described in Materials and methods. (**b**) Oncogenic *ras* increased PPP1CA protein levels. PPP1CA protein levels were analyzed by western blot as described in Materials and methods. (**c** and **d**) Characterization of the effect of PPP1CA downregulation in the DNA damage response to doxorubicin (c) and H_2O_2 (d). NIH cells carrying the shRNA against PPP1CA (shRNA) or vector alone (empty vector) were grown exponentially. Cells were starved and protein levels analyzed by immunoblotting. Western blots of p53, p21, and α-tubulin proteins were analyzed as described in Materials and methods. Concentrations of 0.4 and 0.8 μg/ml doxorubicin during 8 and 24 h were used. In (d) cells were treated with 100 μM H_2O_2, during 6 h. (**e**) Downregulation of PPP1CA inhibits p53-induced pRb hypophosphorylation. In all, 6×10^5 p53−/−;ts-ras cells carrying the shRNA against PPP1CA (shRNA) or vector alone were grown at restricted temperature (39°C) or permissive temperature (32°C) as indicated, during 16 or 24 h. Then, cells were processed for western blot showing hyperphosphorylated (ppRb) and hypophosphorylated (pRb) forms of the protein. α-Tubulin was used as a loading control. The data are representative of three independent experiments. Below, ratio ppRb/pRb is quantified by densitometry. As control, NIH3T3 growing at 37°C is treated with insulin (insulin transferin selenium, ITS) or deprived of serum for 24 h (fetal bovine serum, FBS).

temperature. On the contrary, p53−/−;ts-ras cells stably transduced with shRNA against PPP1CA showed an increase in the hyperphosphorylated form of Rb protein when kept for 16 or 24 h at 32°C (Figure 2e and f). Our data show that downregulation of PPP1CA maintains pRb in the hyperphosporylated state even in the presence of active p53 and, therefore, allowing cell growth.

Oncogenic ras raises endogenous ceramide levels

PPP1CA is regulated by many factors but, among the second messengers that could be activated by oncogenic *ras*, we found that ceramide induction is able to inactivate PP1α (20,21). Ceramide modulates different cellular responses to stress, including apoptosis, cell-cycle arrest and senescence. Raising the intracellular ceramide concentration is sufficient to induce many of these stress responses (21). Therefore, we tested if oncogenic *ras* was able to induce ceramides and whether this induction was related to the features of senescence observed in our system.

We labeled p53−/−;ts;ras and p53−/−;ts cells with [^{14}C]serine and grew them either at 39°C or 32°C during 48 h. Then, we processed the lipidic content to identify the ceramides. Sphingomyelin (one of the ceramide precursors), whose levels were maintained relatively constant, was used to normalize ceramide levels. The measurement of intracellular ceramide levels in our system showed a clear increase of this lipid in the presence of *ras* compared with p53−/−;ts cells (Figure 3a). Normalization against sphingomyelin shows significant increase of ceramides in the presence of oncogenic *ras* both when the cells were growing at 39°C and after 24 h at 32°C. Moreover, although ceramides greatly decrease when the cells arrest at 32°C, in the presence of Ras, ceramide levels only show a small decrease at 32°C and are maintained still higher than in cells growing at 39°C. Therefore, *ras* induced an increase of the levels of ceramide that were maintained even in the presence of active p53.

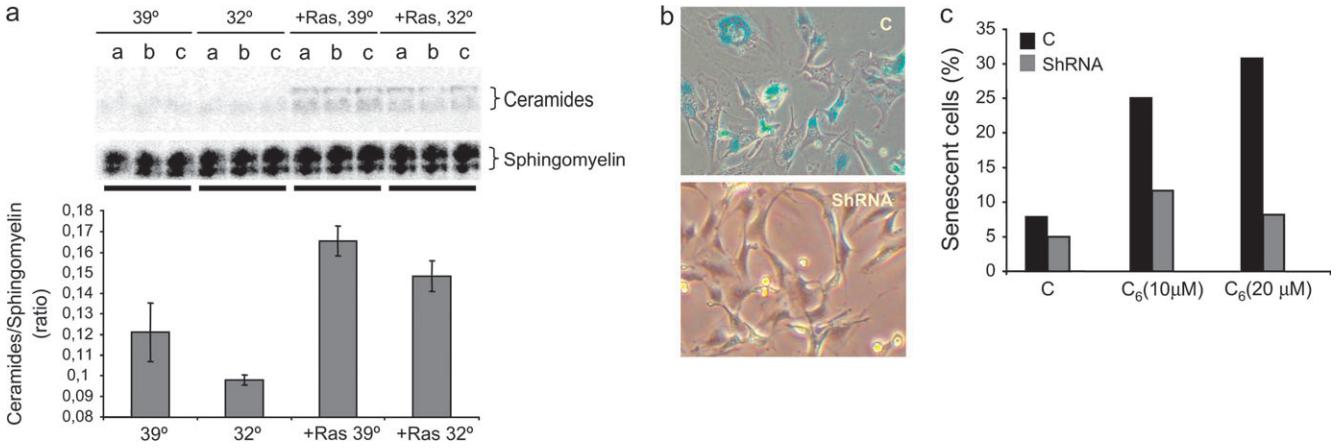

Fig. 3. (**a**) Measurement of intracellular ceramide levels. Ceramides levels were measured as indicated in Materials and methods. Ceramides and sphingomyelin bands are shown. (**a–c**) Triplicates of the same condition. Below, radioactivity corresponding to ceramides and sphingomyelin was automatically quantified by an electronic radiography system (Instantimager). Ceramide values were normalized against sphingomyelin. Results shown are the mean values of a single experiment performed in triplicate, representative of two independent experiments with similar results. (b and c) Effect of exogenous C_6 ceramide addition. p53−/−;ts cells (C) or p53−/−;ts-expressing PPP1CA shRNA cells (shRNA), at 32°C, were treated with 10 or 20 μM C_6-ceramide (*N*-hexanoylsphingosine) (from Biomol). Seventy-two hours after the first ceramide addition, cells were fixed with 0.5% glutaraldehyde in phosphate-buffered saline and senescent morphology was assessed under the microscope. The figure is representative of different independent experiments performed. (c) Quantification of the number of senescent cells observed in the culture after the addition of C6 ceramide. Data are presented as percentage of total cells analyzed. A minimum of 100 cells were analyzed in each of the three independent experiments.

Although little is known about signaling pathways mediated by lipids that lead to senescence, it is a fact that endogenous ceramide levels are markedly and specifically (compared with other lipids) elevated in senescence cells and that exogenous ceramide is able to induce a senescent phenotype in young human diploid fibroblast at concentrations that mimic endogenous levels in senescent cells (22).

We next explored whether the increase of ceramides can be connected to senescence and PPP1CA. To that end, we added soluble C6 ceramide to p53−/−;ts cells stably transfected either with an empty vector or a PPP1CA shRNA. Adding a micromolar concentration of C6 to arrested cells, their senescent morphology increased (Figure 3b and c). However, the expression of an shRNA against PPP1CA inhibits the shift to senescence observed after addition of exogenous C6 ceramide. Therefore, in our system, exogenous soluble ceramide behave as oncogenic *ras*: it switches the phenotype from arrest to senescence, and this effect is inhibited by an shRNA against PPP1CA. Ceramide activates PP1α (20,21) among other phosphatases, leading to growth arrest. In our system, PPP1CA seems to be a mediator of the ceramide-induced growth stop of stressed cells since PPP1CA shRNA inhibits this effect.

PPP1CA as a tumor suppressor?

If reductions in the PPP1CA protein levels are able to bypass p53-induced growth arrest, then PPP1CA could behave as a tumor suppressor. Therefore, loss of PPP1CA should be favored in some tumors. To test this possibility, we hybridized an RNA dot blot array of tumor/normal tissue matched samples from the same patient to measure PPP1CA mRNA. As an expression control, we also hybridized the arrays with an ubiquitin-specific probe, normalized the signals of the specific probes against the signal of ubiquitin and quantitated the signal in tumor and normal samples. We identified those tumor samples in which the signal was decreased by at least 50% with respect to normal tissue (Figure 4a). We found that the amount of PPP1CA mRNA had a marked reduction in several tumor samples. An especially high percentage of tumoral samples with at least a 50% reduction of the PPP1CA mRNA was seen in vulva, prostate, small intestine and kidney tumors (Figure 4a). The percentage of tumors that show reduced levels of PPP1CA mRNA was statistically significant in these four types.

To complement these studies, we have performed a quantitative analysis of the expression of PPP1CA mRNA in lung tumors. We quantified the mRNA in matched tumoral/normal tissue samples of the same patient (Figure 4b). Our data show that PPP1CA mRNA level is lost to a 50% of the control in 20% of tumor samples ($P < 0.05$).

Further we wanted to investigate whether PPP1CA, identified in our loss-of-function screening, was a subject of allelic loss in cancer. PPP1CA is located at 11q13 (23). Due to the evidence that PP1α is a tumor suppressor gene and because it localizes to 11q13, PPP1CA is a candidate gene for type I multiple endocrine neoplasia, which has a susceptibility gene that maps to the same chromosomal region. Translocations involving break points at 11q13 have been observed in lymphomas, chronic lymphocytic leukemia of the B-cell type and multiple myeloma. Therefore, we have explored whether this gene is the putative tumor suppressor localized to this loci. To that end, we analyzed the allelic losses of this gene in DNA from tumor samples of different origins. We analyzed samples from thyroid ($n = 14$), kidney ($n = 6$, all clear-cell renal carcinoma), larynx ($n = 14$) and colon ($n = 15$). Analysis of specific PPP1CA genomic loss showed single allelic losses in all the tumor types analyzed (Figure 4c) with variations in frequency among tumor types. However, only in kidney and colorectal cancer the percentage of tumors showing allelic loss was statistically significant, correlating with previous data of mRNA downregulation in these two tumor types.

Overexpression of a fragment of PPP1CA cDNA reduces the malignant properties of tumor cells

There exist different splicing variants of PPP1CA (Figure 5a) whose presence in p53−/−;ts MEFs and p53−/−;ts;ras MEFs (Ras) was confirmed by specific RT–PCR (Figure 5b). Five of these variants were cloned into the pBabepuro vector and were overexpressed in human HCT116 p53−/− colon cancer cells to assess their possible differential effects. Overexpression of the SP1 fragment significantly reduced the number of colonies that were able to grow. Nevertheless, with SP0 (the complete cDNA), only a moderate effect was observed (Figure 5c). The growth inhibitory effect was not observed when the SP3, SP5 and SP6 splicing forms were overexpressed (data not shown). Individual senescent cells were observed in HCT116 after transfection with SP0 and SP1 splicing variants. Similar observations were made in p53−/−;ts-ras cells (data not shown).

Next, we selected a population of HCT116 cells expressing the PPP1CA SP0 and SP1 variants and seeded them in soft agar to test

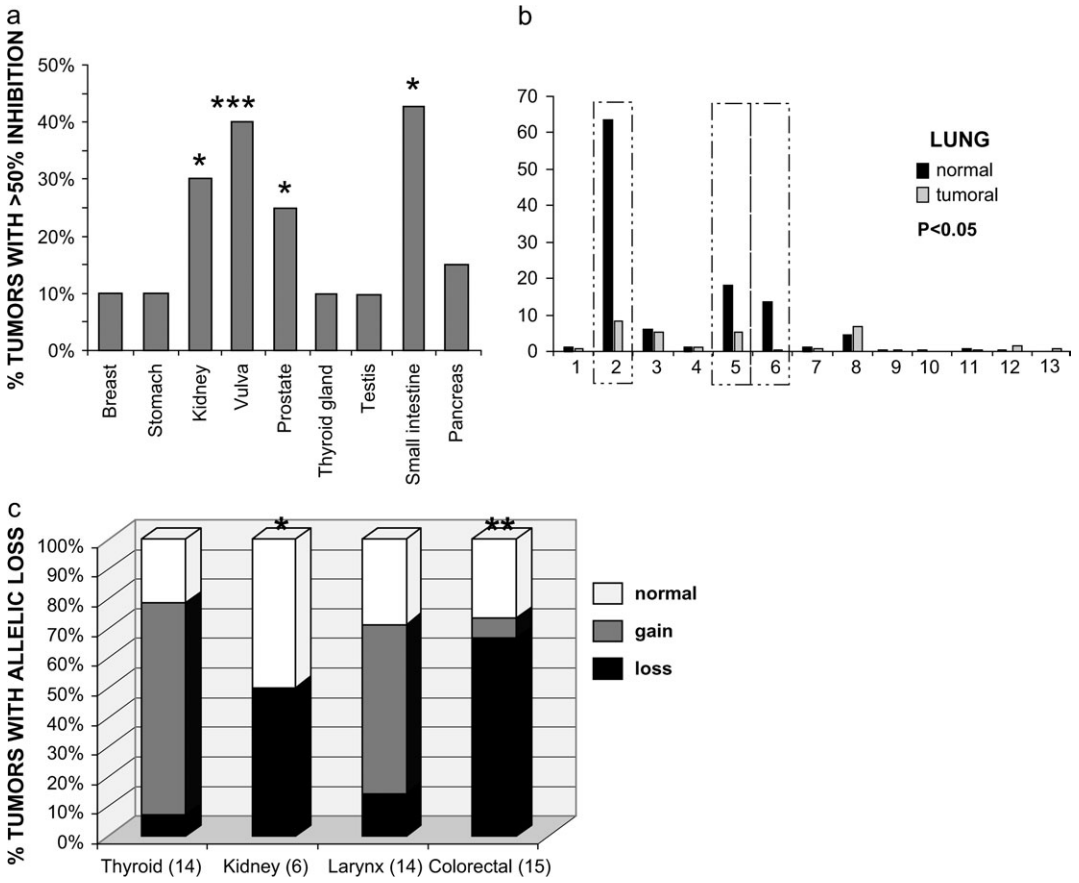

Fig. 4. (**a**) Percentage of tumor samples showing decreased levels of mRNA. Cancer Profiling Array membranes (BD Biosciences) with paired non-tumoral/tumoral samples from the same patient were hybridized with P32-labeled probes of the genes of interest to determine the respective amount of mRNAs. This figure shows relative amount of repressed samples (>50%) for each type of tumor in relation to their paired sample of normal tissue (black). (**b**) Expression of the genes of interest is reduced in some tumoral samples with respect to non-tumoral samples of the same patient. mRNA present in tumors versus non-tumoral samples from the same patient was analyzed in 13 or 16 patients of colon and lung tumors by Q-RT–PCR. (**c**) Analysis of genomic loses for Csn2 and BRF1. Percentage of tumors showing allelic loss in each type of tumor. Statistical analysis was performed by unpaired *t*-test comparing against the percentage of samples that show >50% increase in normal samples versus tumoral samples of the same patient (a and b), against the frequency of allelic loss in non-tumoral samples (c). $^{*}P < 0.05$; $^{**}P < 0.005$; $^{***}P < 0.001$.

their ability to grow in semisolid media. We observed that cells which overexpressed PPP1CA grew worse in soft agar, forming fewer colonies and smaller in size (Figure 5d).

These results are in agreement with the ones reported by other authors (17) that showed how a constitutively active mutant PP1α, unable to be inactivated by phosphorylation, arrests cell growth in G_1, whereas wild-type PP1α, presumably suffering this inhibitory phosphorylation by cyclin-dependent kinases, does not arrest cell growth. This can be explained because full-length PP1α has a residue (Thr320) that can suffer inhibitory phosphorylation by cyclin-dependent kinases (24), whereas the SP1 variant, that encodes a shorter protein, does not have this residue but still keeps the serine/threonine-specific protein phosphatase domain.

Reduction of PPP1CA levels increases malignant properties of tumor cells

Our previous data suggested that PPP1CA could be a putative tumor suppressor. Therefore, we decided to test whether downregulation of the PPP1CA signal might have influence in the malignant behavior of tumor cells. To that end, we generated three shRNAs against human PPP1CA and tested them in HCT116 cells. We stably selected cell populations expressing each of the shRNAs and analyzed the amount of PPP1CA protein. All three shRNAs halved the levels of PPP1CA protein (Figure 6a). Later, we analyzed whether this reduction had any influence in the malignant behavior of the transfected cells. In fact, cells with reduced levels of PPP1CA grew better in soft agar generating higher number of colonies and of bigger size (Figure 6b).

Discussion

We have used an antisense-based systematic approach to uncover genes that are important for the onset of ras/p53-dependent cellular senescence. Together with antisenses against p53 (that constitute a validation for our screening), we have found several antisense fragments against genes of known and unknown functions. Among them, an antisense fragment against PPP1CA (PP1 catalytic subunit, α isoform) that bypassed the *ras*/p53-induced arrest in MEFs.

Protein phosphorylation at serine and threonine residues is a crucial step in the regulation of many cellular functions ranging from hormonal signaling to cell division and even short-term memory. The level of protein phosphorylation in a signaling cascade is controlled by the opposing actions of protein kinases and protein phosphatases. PP1 is one of four major serine/threonine-specific protein phosphatases identified in eukaryotic cells by enzymatic methods. Although the four majoritary cellular phosphatases have overlapping substrate specificities *in vitro*, they show higher specificities *in vivo*. There are four different isoforms of the PP1 catalytic subunit (α, β, γ1 and γ2) and each of them can bind to many non-substrate cellular proteins that function as regulatory subunits (25). These subunits modify the activity of PP1 and/or target it to particular substrates. The PPP1CA gene

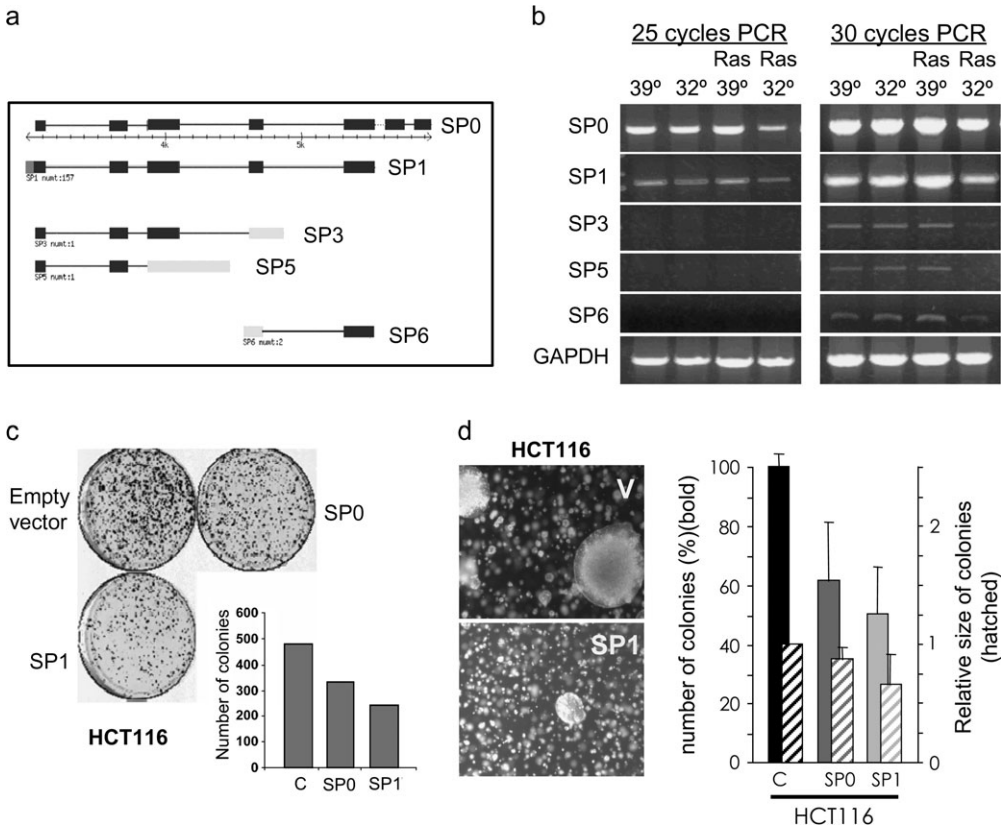

Fig. 5. Effect of overexpression of different splicing variants of PPP1CA. (**a**) The diagram shows the different PPP1CA splicing variants predicted by computer programs. In red are the primers to specifically amplify each variant. (**b**) The existence of the different splice pattern sequences was confirmed by specific RT–PCR in p53−/−;ts MEFs and p53−/−;ts;ras (Ras) MEFs. All the splice variants appeared in the different conditions of temperature, although at different levels of expression. SP0 and SP1 are the predominant variants. (**c**) SP1 fragment of PPP1CA reduced significantly the growth of colonies in HCT116 p53−/− cells. SP0 exerted only a moderate effect reducing the number of colonies able to grow. HCT116 p53−/− cells were infected with viruses carrying each one of the splicing variant in pBabepuro vector or vector alone. After selection, 5×10^3 cells were seeded per 10 cm dish. After 10 days, cells were fixed and stained and colonies counted. (**d**) SP1 and SP0 splicing variants reduced the growth in soft agar. Cells (10^4) were cultured following the procedure described in Materials and methods, 4 weeks later they were fixed and pictures taken. The images shown are representative of different independent experiments performed. V, cells carrying empty vector; HCT116, cells carrying the SP1 splicing variant. For the quantification: bold, number of colonies; data presented are the mean from triplicate samples; bars, ±standard deviation; hatched, colony size was determined by measuring a minimum of 30 representative colonies.

code for the catalytic subunit of the PP1α isoform, together with regulatory subunits, forms PP1α (23). The PP1 catalytic subunits are rarely found alone in nature. Rather, higher order structures of PP1 are formed by oligomerization with regulatory subunits. This ensures multiple possibilities for the regulation and direction of PP1 activity in response to signal transduction stimuli. Through the existence of multiple regulatory subunits, each of them with the possibility of being modified, PP1 activity can be quickly and decisively regulated (18).

Barker *et al.* (23) mapped the PPP1CA gene to 11q13 by Southern analysis of somatic cell hybrids and by *in situ* hybridization. Due to the accumulated evidence that PP1α functions as a tumor suppressor and that PPP1CA maps to the same chromosomal region than the gene responsible for type I multiple endocrine neoplasia, PPP1CA has been proposed as a candidate gene for type I multiple endocrine neoplasia. Translocations involving break points at 11q13 have been observed also in lymphoma, chronic lymphocytic leukemia of the B-cell type and multiple myeloma.

PP1α is one of the major cellular phosphatases involved in pRB dephosphorylation (19,26–29). We propose that oncogenic *ras*–induced ceramides contribute to the permanent growth arrest observed in senescence by activating PPP1CA and therefore maintaining pRb in its hypophosphorylated state. Therefore, downregulation of PPP1CA bypasses oncogenic stress–induced senescence and might contribute to tumorigenesis by impairing pRb phosphorylation.

pRB-specific PP1α phosphatase activity is regulated in a different way when cells are normally progressing through the cell cycle than when cells are cell-cycle arrested under stress conditions. Phosphatase nuclear targeting subunit is a PP1 regulatory subunit that specifically inhibits retinoblastoma-directed PP1 activity (30). Thus, PP1–phosphatase nuclear targeting subunit association persist as cells progress through the cell cycle, but during cellular stress phosphatase nuclear targeting subunit dissociates from PP1 and consequently the threonine 821 of pRb is dephosphorylated (31) and cells are arrested in G_1. This process is concurrent with our observations of growth inhibition by the SP1 splicing variant of PPP1CA.

PP1α has the potential to arrest cells in the G_1 phase of the cell cycle unless PP1α itself is inactivated by periodic phosphorylation at Thr320, presumably by the cyclin-dependent kinases that regulate G_1–S transition. In fact, a constitutively active PP1α mutant that is resistant to phosphorylation causes pRb-dependent G_1 arrest in human cancer cells (17).

In our system, oncogenic *ras* promotes an increase in the intracellular levels of ceramides and a concomitant *ras*-dependent increase in PPP1CA protein level and activity, measured as pRB dephosphorylation. Ceramide modulates a number of biochemical and cellular responses to stress, including apoptosis, cell-cycle arrest and cellular senescence. Raising the intracellular ceramide concentration is sufficient to induce many of these stress responses (21).

Although there are several signaling pathways that include ceramide as the final messenger that triggers cellular apoptosis, little is known about lipid-mediated signaling pathways that lead to senescence. Nevertheless, endogenous ceramide levels are markedly and

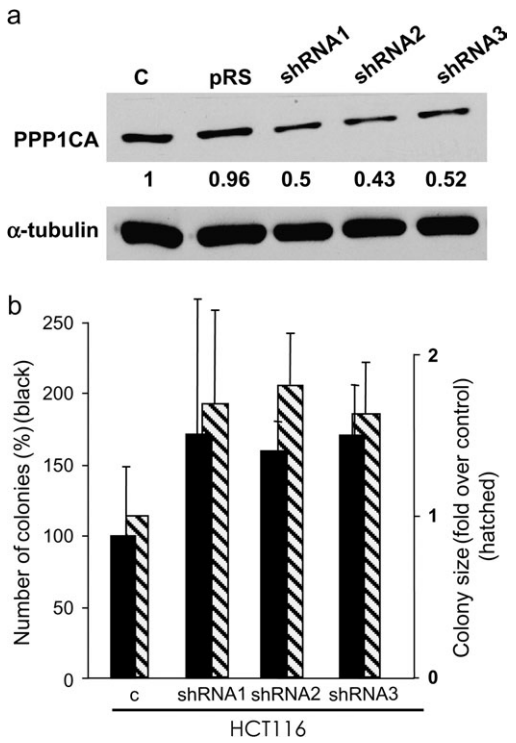

Fig. 6. Downregulation of PPP1CA increases growth in soft agar of HCT116. (**a**) Effect of shRNAs against human PPP1CA. HCT116 cells carrying the shRNA against PPP1CA (shRNA) or vector alone (pRS) were grown exponentially. Cells were starved and protein levels analyzed by immunoblotting. (**b**) PPP1CA shRNA increased growth in soft agar. Cells (10^4) were cultured following the procedure described in Materials and methods, 4 weeks later they were fixed, and number of colonies counted. C, cells carrying empty vector; bold, number of colonies; data presented are the mean from triplicate samples; bars, ±standard deviation; hatched, colony size was determined by measuring a minimum of 30 representative colonies.

specifically elevated in senescence cells. Furthermore, exogenous ceramide is able to induce a senescent phenotype, increasing the expression of the senescence histochemical marker β-galactosidase in young human diploid fibroblast at concentrations that mimic endogenous levels in senescent cells (22). Taking into account that ceramide is able to induce pRb hypophosphorylation leading to growth arrest and cellular senescence and that ceramide activated both protein phosphatase 1 and protein phosphatase 2A (20,32), we could suppose that ceramide induction of Rb hypophosphorylation is mediated, at least partly, by PPP1CA (32). And this matches perfectly with the fact that ceramide-induced dephosphorylation of Rb is selectively inhibited by inhibitors of PP1 (21,33,34).

We propose that oncogenic *ras* might be one of the stress agents that cause ceramide to accumulate, thereby activating PP1α and maintaining pRb hypophosphorylated. It has been described that PP1α is a Ras-activated phosphatase (14), and we have observed that Ras increases PPP1CA protein level in two different cell types. We also observed a clear p53-dependent increase of PPP1CA protein level, suggesting that p53 might be important for the onset of the *ras*-induced senescence, since a higher amount of more active PPP1CA can keep pRB in a dephosphorylated state. Other authors have shown that p53 is necessary for ceramide accumulation and pRB dephosphorylation after DNA damage (35). In our hands, p53 is not essential for the Ras-dependent accumulation of ceramides and subsequent activation of PP1α, but can contribute to the establishment of senescence increasing the amount of PPP1CA. It is tempting to think that, when oncogenic Ras is sensed as a cellular stress, ceramide functions as a tumor suppressor lipid (36).

Supporting this hypothesis, a reduction in the PPP1CA expression by shRNA impaired cellular senescence induced by exogenous ceramides. Furthermore, we have also observed a decrease in cell number in cultures carrying PPP1CA shRNA (data not shown) probably due to other PP1α activities in these cells such as Bad dephosphorylation and triggering of apoptosis (14,17). Moreover, a reduction of the PPP1CA level increases the malignant properties of the tumoral cells, and in turn, overexpression of the SP1 splice variant of PPP1CA reduced such malignant properties.

Finally, our data reinforce previous works suggesting that PPP1CA might behave as a tumor suppressor under certain conditions (14,37,38). Our analysis of human tumor samples showed a percentage of tumors with downregulation of PPP1CA, in some cases due to genomic loss. Although these data are preliminary and need further confirmation, they open the possibility that PP1 regulatory proteins might also behave as specific tumor suppressors under certain conditions.

Funding

Fondo de Investigación Sanitaria (FIS-02/0126); Ministerio de Ciencia y Tecnología (SAF2005-00944); Fundación Mutua Madrileña and European Union (from VI framework, Project COMBIO); Ministerio de Ciencia y Tecnología to M.E.C.

Acknowledgements

We thank Juan Carlos Lacal's group, and specially Sara Bertrand, for the helpful assistance with the 'Measurement of intracellular ceramide levels' technique.

Conflict of Interest Statement: None declared.

References

1. Serrano,M. *et al*. (1997) Oncogenic ras provokes premature cell senescence associated with accumulation of p53 and p16INK4a. *Cell*, **88**, 593–602.
2. Lin,A.W. *et al*. (1998) Premature senescence involving p53 and p16 is activated in response to constitutive MEK/MAPK mitogenic signaling. *Genes Dev.*, **12**, 3008–3019.
3. de Stanchina,E. *et al*. (1998) E1A signaling to p53 involves the p19(ARF) tumor suppressor. *Genes Dev.*, **12**, 2434–2442.
4. Ferbeyre,G. *et al*. (2002) Oncogenic ras and p53 cooperate to induce cellular senescence. *Mol. Cell. Biol.*, **22**, 3497–3508.
5. Palmero,I. *et al*. (1998) p19ARF links the tumour suppressor p53 to Ras. *Nature*, **395**, 125–126.
6. Sherr,C.J. *et al*. (2000) The ARF/p53 pathway. *Curr. Opin. Genet. Dev.*, **10**, 94–99.
7. Mayo,L.D. *et al*. (2002) The PTEN, Mdm2, p53 tumor suppressor-oncoprotein network. *Trends Biochem. Sci.*, **27**, 462–467.
8. Sionov,R.V. *et al*. (1999) The cellular response to p53: the decision between life and death. *Oncogene*, **18**, 6145–6157.
9. Castro,M.E. *et al*. (2004) Cellular senescence induced by p53-ras cooperation is independent of p21waf1 in murine embryo fibroblasts. *J. Cell. Biochem.*, **92**, 514–524.
10. Carnero,A. *et al*. (2000) Loss-of-function genetics in mammalian cells: the p53 tumor suppressor model. *Nucleic Acids Res.*, **28**, 2234–2241.
11. Guijarro,M.V. *et al*. (2007) MAP17 enhances the malignant behaviour of tumor cells through ROS increase. *Carcinogenesis*, **28**, 2096–2104.
12. Guijarro,M.V. *et al*. (2007) MAP17 overexpression is a common characteristic of carcinomas. *Carcinogenesis*, **28**, 1646–1662.
13. Schouten,J.P. *et al*. (2002) Relative quantification of 40 nucleic acid sequences by multiplex ligation-dependent probe amplification. *Nucleic Acids Res.*, **30**, e57.
14. Ayllon,V. *et al*. (2000) Protein phosphatase 1alpha is a Ras-activated Bad phosphatase that regulates interleukin-2 deprivation-induced apoptosis. *EMBO J.*, **19**, 2237–2246.
15. Rajesh,D. *et al*. (1999) Ras mutation, irrespective of cell type and p53 status, determines a cell's destiny to undergo apoptosis by okadaic acid, an inhibitor of protein phosphatase 1 and 2A. *Mol. Pharmacol.*, **56**, 515–525.
16. Nelson,D.A. *et al*. (1997) High molecular weight protein phosphatase type 1 dephosphorylates the retinoblastoma protein. *J. Biol. Chem.*, **272**, 4528–4535.

17. Berndt,N. *et al*. (1997) Constitutively active protein phosphatase 1alpha causes Rb-dependent G1 arrest in human cancer cells. *Curr. Biol.*, **7**, 375–386.
18. Rubin,E. *et al*. (1998) Protein phosphatase type 1, the product of the retinoblastoma susceptibility gene, and cell cycle control. *Front. Biosci.*, **3**, D1209–D1219.
19. Alberts,A.S. *et al*. (1993) Regulation of cell cycle progression and nuclear affinity of the retinoblastoma protein by protein phosphatases. *Proc. Natl Acad. Sci. USA*, **90**, 388–392.
20. Lee,J.Y. *et al*. (2000) Regulation of cyclin-dependent kinase 2 activity by ceramide. *Exp. Cell Res.*, **261**, 303–311.
21. Hannun,Y.A. *et al*. (2000) Ceramide in the eukaryotic stress response. *Trends Cell Biol.*, **10**, 73–80.
22. Venable,M.E. *et al*. (1995) Role of ceramide in cellular senescence. *J. Biol. Chem.*, **270**, 30701–30708.
23. Barker,H.M. *et al*. (1990) Localization of the gene encoding a type I protein phosphatase catalytic subunit to human chromosome band 11q13. *Genomics*, **7**, 159–166.
24. Liu,C.W. *et al*. (1999) Inhibitory phosphorylation of PP1alpha catalytic subunit during the G(1)/S transition. *J. Biol. Chem.*, **274**, 29470–29475.
25. Damer,C.K. *et al*. (1998) Rapid identification of protein phosphatase 1-binding proteins by mixed peptide sequencing and data base searching. Characterization of a novel holoenzymic form of protein phosphatase 1. *J. Biol. Chem.*, **273**, 24396–24405.
26. Ludlow,J.W. *et al*. (1993) Specific enzymatic dephosphorylation of the retinoblastoma protein. *Mol. Cell. Biol.*, **13**, 367–372.
27. Yan,Y. *et al*. (1999) Distinct roles for PP1 and PP2A in phosphorylation of the retinoblastoma protein. PP2a regulates the activities of G(1) cyclin-dependent kinases. *J. Biol. Chem.*, **274**, 31917–31924.
28. Rubin,E. *et al*. (2001) Site-specific and temporally-regulated retinoblastoma protein dephosphorylation by protein phosphatase type 1. *Oncogene*, **20**, 3776–3785.
29. Wang,R.H. *et al*. (2001) Protein phosphatase 1alpha-mediated stimulation of apoptosis is associated with dephosphorylation of the retinoblastoma protein. *Oncogene*, **20**, 6111–6122.
30. Udho,E. *et al*. (2002) PNUTS (phosphatase nuclear targeting subunit) inhibits retinoblastoma-directed PP1 activity. *Biochem. Biophys. Res. Commun.*, **297**, 463–467.
31. Krucher,N.A. *et al*. (2006) Dephosphorylation of Rb (Thr-821) in response to cell stress. *Exp. Cell Res.*, **312**, 2757–2763.
32. Chalfant,C.E. *et al*. (1999) Long chain ceramides activate protein phosphatase-1 and protein phosphatase-2A. Activation is stereospecific and regulated by phosphatidic acid. *J. Biol. Chem.*, **274**, 20313–20317.
33. Kishikawa,K. *et al*. (1999) Phosphatidic acid is a potent and selective inhibitor of protein phosphatase 1 and an inhibitor of ceramide-mediated responses. *J. Biol. Chem.*, **274**, 21335–21341.
34. Ruvolo,P.P. (2003) Intracellular signal transduction pathways activated by ceramide and its metabolites. *Pharmacol. Res.*, **47**, 383–392.
35. Dbaibo,G.S. *et al*. (1998) p53-dependent ceramide response to genotoxic stress. *J. Clin. Invest.*, **102**, 329–339.
36. Hannun,Y.A. (1994) The sphingomyelin cycle and the second messenger function of ceramide. *J. Biol. Chem.*, **269**, 3125–3128.
37. Dessauge,F. *et al*. (2006) Identification of PP1alpha as a caspase-9 regulator in IL-2 deprivation-induced apoptosis. *J. Immunol.*, **177**, 2441–2451.
38. Liu,C.W. *et al*. (2006) Protein phosphatase 1alpha activity prevents oncogenic transformation. *Mol. Carcinog.*, **45**, 648–656.

Received August 29, 2007; revised October 25, 2007; accepted October 27, 2007